



**HAL**  
open science

## **Pathogenic Bacteria Induce Colonic PepT1 Expression: An Implication in Host Defense Response**

Hang Thi Thu Nguyen, Guillaume Dalmaso, Kimberly R Powell, Yutao Yan, Shantanu Bhatt, Daniel Kalman, Shanthi V Sitaraman, Didier Merlin

### ► **To cite this version:**

Hang Thi Thu Nguyen, Guillaume Dalmaso, Kimberly R Powell, Yutao Yan, Shantanu Bhatt, et al.. Pathogenic Bacteria Induce Colonic PepT1 Expression: An Implication in Host Defense Response. *Gastroenterology*, 2009, 137, pp.1435 - 1447.e2. <10.1053/j.gastro.2009.06.043>. <hal-04653405>

**HAL Id: hal-04653405**

**<https://hal.science/hal-04653405v1>**

Submitted on 13 Mar 2025

**HAL** is a multi-disciplinary open access archive for the deposit and dissemination of scientific research documents, whether they are published or not. The documents may come from teaching and research institutions in France or abroad, or from public or private research centers.

L'archive ouverte pluridisciplinaire **HAL**, est destinée au dépôt et à la diffusion de documents scientifiques de niveau recherche, publiés ou non, émanant des établissements d'enseignement et de recherche français ou étrangers, des laboratoires publics ou privés.



HAL Authorization

## Pathogenic Bacteria Induce Colonic PepT1 Expression: An Implication in Host Defense Response

HANG THI THU NGUYEN,\* GUILLAUME DALMASSO,\* KIMBERLY R. POWELL,† SHANTANU BHATT,† DANIEL KALMAN,† SHANTHI V. SITARAMAN,\* and DIDIER MERLIN\*

\*Department of Medicine and †Department of Pathology, Emory University, Atlanta, Georgia

**BACKGROUND & AIMS:** Expression of the di/tripeptide transporter PepT1 has been observed in the colon under inflammatory conditions; however, the inducing factors and underlying mechanisms remain unknown. Here, we address the effects of pathogenic bacteria on colonic PepT1 expression together with its functional consequences. **METHODS:** Human colonic HT29-Cl.19A cells were infected with the attaching and effacing enteropathogenic *Escherichia coli* (EPEC). Wild-type and PepT1 transgenic mice or cultured colonic tissues derived from these mice were infected with *Citrobacter rodentium*, a murine attaching and effacing pathogen related to EPEC. **RESULTS:** EPEC induced PepT1 expression and activity in HT29-Cl.19A cells by intimately attaching to host cells through lipid rafts. Induction of PepT1 expression by EPEC required the transcription factor Cdx2. PepT1 expression reduced binding of EPEC to lipid rafts, as well as activation of nuclear factor- $\kappa$ B and mitogen-activated protein kinase and production of interleukin-8. Accordingly, *ex vivo* and *in vivo* experiments revealed that *C. rodentium* induced colonic PepT1 expression and that, compared with their wild-type counterparts, PepT1 transgenic mice infected with *C. rodentium* exhibited decreased bacterial colonization, production of proinflammatory cytokines, and neutrophil infiltration into the colon. **CONCLUSIONS:** Our findings demonstrate a molecular mechanism underlying the regulation of colonic PepT1 expression under pathologic conditions and reveal a novel role for PepT1 in host defense via its capacity to modulate bacterial-epithelial interactions and intestinal inflammation.

The di/tripeptide transporter PepT1 is normally expressed in the brush border membranes of enterocytes in the small intestine, the proximal tubular cells of the kidney, the bile duct epithelial cells, and the immune cells.<sup>1</sup> It has been reported that PepT1 expression is induced in colonic epithelial cells under inflammatory conditions<sup>2,3</sup> and that PepT1 can mediate the transport of bacterial proinflammatory peptides into colonic epithelial cells.<sup>1</sup> Although the mechanism of PepT1 expression under pathologic conditions remains unknown, it has been suggested that PepT1 expression is likely in-

duced at a transcriptional level and that specific transcriptional regulation by signaling pathway(s) may be activated.<sup>2-5</sup> We previously showed that PepT1 is localized in lipid rafts (LRs) of intestinal epithelial cells (IECs) and immune cells.<sup>6</sup> LR s have been proposed to compartmentalize proteins and lipids to regulate many cellular functions, such as sorting and trafficking of proteins and signal transduction.<sup>7</sup> Recently, several lines of evidence have suggested a role for LR s as docking sites for pathogens to attack host cells.<sup>8,9</sup>

Enteropathogenic *Escherichia coli* (EPEC) is a food-borne pathogen that is implicated in the pathophysiology of infantile diarrhea.<sup>10</sup> EPEC intimately attaches to host IECs through the binding of the bacterial outer membrane protein intimin to Tir, a bacterium-encoded factor translocated into the host plasma membrane upon infection. Attachment of EPEC causes attaching and effacing lesions, characterized by formation of actin-filled membranous protrusions (pedestal) and destruction of microvilli.<sup>11</sup> EPEC also induces inflammatory responses in IECs, characterized by activation of nuclear factor (NF)- $\kappa$ B<sup>12</sup> and mitogen-activated protein kinases<sup>13,14</sup> and production of proinflammatory cytokines, such as interleukin (IL)-8.<sup>13,14</sup> EPEC has been reported to affect epithelial membrane transport activities, including butyrate uptake,<sup>15</sup> Na<sup>+</sup>/H<sup>+</sup> exchange,<sup>16</sup> and Cl<sup>-</sup>/OH<sup>-</sup> exchange.<sup>17</sup> These activity changes are suggested to be consequences of the redistribution of surface proteins from the apical membranes into the intracellular compartments.<sup>15,17</sup> However, the transcriptional mechanisms underlying regulation of membrane transport by EPEC remain unknown.

Here, we address (1) the role of EPEC in the induction of PepT1 expression and function in colonic epithelial cells, (2) the molecular mechanisms underlying EPEC-induced PepT1 expression, and (3) the role of colonic PepT1 in bacterial-epithelial interactions and bacteria-

**Abbreviations used in this paper:** ChIP, chromatin immunoprecipitation; EPEC, enteropathogenic *Escherichia coli*; IECs, intestinal epithelial cells; KC, keratinocyte-derived chemokine; KPV, Lysine-Proline-Valine; LR s, lipid rafts.

© 2009 by the AGA Institute  
0016-5085/09/\$36.00  
doi:10.1053/j.gastro.2009.06.043

induced intestinal inflammation. In vitro studies were validated by ex vivo and in vivo experiments using a PepT1 transgenic mouse model and *Citrobacter rodentium*, a murine attaching and effacing pathogen closely related to EPEC, which has been shown to produce comparable ultrastructural changes in mouse distal colons.<sup>18,19</sup>

## Materials and Methods

### Cell Culture and In Vitro Infection

HT29-Cl.19A cells were grown in Dulbecco's modified Eagle medium (DMEM) supplemented with 10% fetal bovine serum (FBS) and 1.5  $\mu\text{g}/\text{mL}$  plasmocin. Wild-type (WT) EPEC E2348/69 and EPEC mutant  $\Delta\text{eae}$  and  $\Delta\text{tir}$  strains were grown in Luria-Bertani broth. For infection, EPEC suspension in DMEM was added to confluent cell monolayers with a multiplicity of infection of 10. For adhesion assay, infected cells were washed, lysed, and plated on Luria-Bertani plates.

### Ex Vivo and In Vivo Infection

Eight-week-old FVB WT and PepT1 transgenic mice<sup>20</sup> were used (Supplementary Materials and Methods). *C. rodentium* (ATCC No. S1116) were cultured overnight at 37°C in Luria-Bertani broth.

For ex vivo infection, mouse colonic tissues cultured as described previously<sup>21</sup> were infected with *C. rodentium*. Six hours after infection, supernatants were collected, and specimens were washed with phosphate-buffered saline (PBS).

For infection of mice, food was withdrawn, and drinking water was replaced with *C. rodentium* suspension in 20% sucrose distilled water overnight ( $4 \times 10^8$  colony-forming units [CFU]/mouse) as previously described.<sup>22</sup> Seven days after infection, serum was collected, and mice were killed.

### C. rodentium Colony Counts

Colonic tissue samples were homogenized in 1 mL PBS and plated on MacConkey agar plates. *C. rodentium* colonies were recognized as pink with a white rim as previously described.<sup>23</sup>

### Plasmid Construction and Transfection

Complementary DNA (cDNA) encoding Cdx2 or PepT1 was cloned as previously described.<sup>6,24</sup> HT29-Cl.19A cells were transfected with these constructs using lipofectin (Invitrogen, Grand Island, NY) and stably selected in culture medium containing 1.2 mg/mL geneticin (Invitrogen).

### Isolation of Lipid Rafts From HT29-Cl.19A Cells

HT29-Cl.19A cells were treated or not with 10 mmol/L methyl- $\beta$ -cyclodextrin (m $\beta$ CD) for 30 minutes and replenished with 2 mmol/L cholesterol for 1 hour. Isolation of LRs was performed as previously described.<sup>25</sup>

Briefly, cells were lysed with 1% Triton X-100 in TNE buffer (25 mmol/L Tris-HCl, pH 7.4, 150 mmol/L NaCl, 5 mmol/L EDTA). Lysates were adjusted to 40% sucrose in TNE buffer, overlaid with 2 volumes of 30% sucrose and 1 volume of 5% sucrose, and then centrifuged at 40,000 rpm for 18 hours at 4°C in a Sorval SW 41 Ti rotor (Beckman, Fullerton, CA). Twelve fractions (1 mL each) were collected from the top of the gradient. The floating membrane fraction was defined as LRs.

### Dual-Luciferase Reporter Assay

HT29-Cl.19A cells were transiently transfected with 5 ng of the construct encoding *Renilla* luciferase (Promega, Madison, WI) and 2  $\mu\text{g}$  of PepT1 promoter construct previously cloned<sup>24</sup> using lipofectin. Luciferase activity was detected with a luminometer (Luminoskan; Thermo LabSystems, Beverly, MA) and normalized to *Renilla* luciferase activity.

### Reverse-Transcription Polymerase Chain Reaction and Real-Time Reverse-Transcription Polymerase Chain Reaction

Reverse-transcription polymerase chain reaction (RT-PCR) was performed using GeneJET Fast PCR kit (Fermentas, Glen Burnie, MD). Real-time RT-PCR was performed using iQ SYBR Green Supermix (Bio-Rad, Hercules, CA) and an iCycler (Bio-Rad). Primers used are described in Supplementary Materials and Methods.

### Cloning of Full-Length cDNA Encoding PepT1 Expressed in EPEC-Infected HT29-Cl.19A Cells

Total RNA was isolated from EPEC-infected HT29-Cl.19A cells and reverse transcribed using cDNA Synthesis kit (Fermentas). RT-PCR was performed using Platinum Taq DNA Polymerase (Invitrogen) and specific primers (Supplementary Materials and Methods). The resulting PCR product was cloned into pGEM-T Easy Vector (Promega). Plasmids were grown and purified, and the insert was sequenced (Lark Technologies, Houston, TX).

### Immunofluorescence Staining

HT29-Cl.19A cells on coverslips or filter supports were stained with PepT1 antibody and Alexa Fluor 488-conjugated anti-rabbit secondary antibody (Molecular Probes, Eugene, OR) as previously described.<sup>6</sup>

### Electrophoretic Mobility Shift Assay

Electrophoretic mobility shift assay (EMSA) was performed using biotin-labeled double-stranded oligonucleotide encoding the Cdx2<sup>-579</sup>-binding site-containing PepT1 promoter (Supplementary Materials and Methods). Supershift assay was performed using Cdx2 antibody (Zymed Laboratories, San Francisco, CA).

**Chromatin Immunoprecipitation Assay**

Chromatin immunoprecipitation (ChIP) assay was performed using a ChIP kit (Upstate, Lake Placid, NY). Briefly, after protein-DNA cross-linking, cell lysates were immunoprecipitated using Cdx2 antibody. The immunoprecipitated chromatin was eluted from the protein A, and the cross-linked protein-DNA complexes were reversed. Cdx2<sup>-579</sup>-binding sequence in PepT1 promoter was detected by RT-PCR using specific primers (Supplementary Materials and Methods).

**Nuclear Run-on Assay**

See Supplementary Materials and Methods.

**Western Blot and Dot Blot**

See Supplementary Materials and Methods.

**Uptake Experiments**

PepT1-mediated uptake of [<sup>3</sup>H]Lysine-Proline-Valine (KPV) was performed as previously described.<sup>26</sup> Briefly, confluent HT29-Cl.19A cells were washed, stabilized in HBSS-10 mmol/L HEPES (pH 7.4) for 15 minutes at 37°C, and incubated with 20 nmol/L [<sup>3</sup>H]KPV ± 20 mmol/L glycine-leucine for 15 minutes at room temperature. Cells were washed, and radioactivity was counted in a β-counter (Beckman).

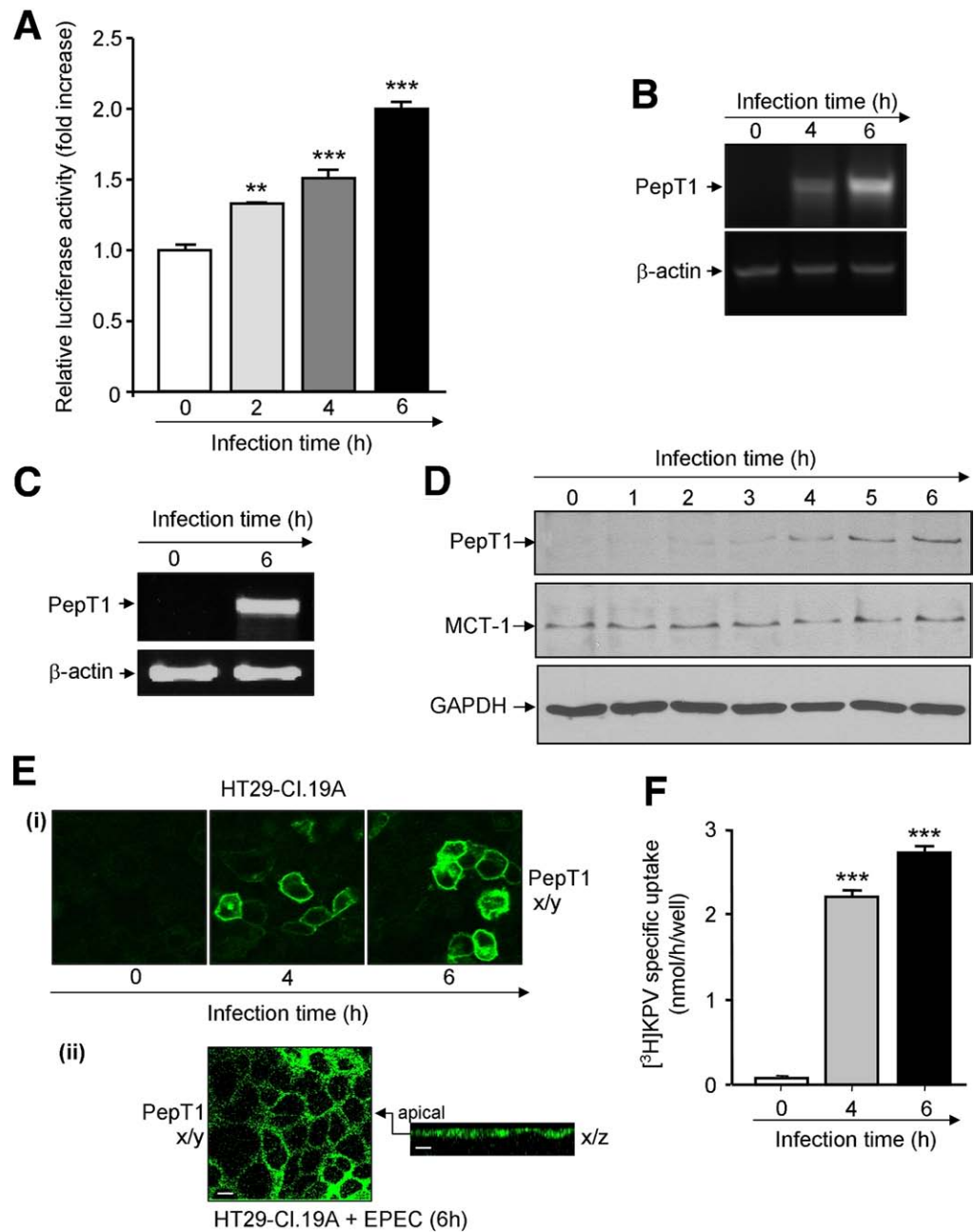


**Figure 1.** EPEC induces PepT1 expression and transport activity in HT29-Cl.19A cells. (A) PepT1 promoter activity assessed by measuring luciferase activity at different time points of EPEC infection (normalized to *Renilla* luciferase activity). (B) PepT1 mRNA expression assessed by RT-PCR. (C) In vitro transcription run-on assay performed on nuclei isolated from uninfected and infected cells. (D) Expression of PepT1 and monocarboxylic transporter-1 (*MCT-1*), used as a control, assessed by Western blot. (E) Representative confocal microscopy images of immunofluorescence staining for PepT1 in nonpolarized HT29-Cl.19A cells on coverslips (i) or polarized cells on filter supports (ii). Bars, 10 μm. (F) PepT1-mediated [<sup>3</sup>H]KPV uptake in HT29-Cl.19A monolayers. Data are means ± SEM of 3 determinations. \*\**P* < .005; \*\*\**P* < .001 vs uninfected cells.

**Measurement of EPEC Attachment to Lipid Rafts**

EPEC attachment was monitored using the electric cell-substrate impedance sensing 1600R device (Applied BioPhysics, Troy, NY). EPEC was seeded in electric cell-substrate impedance sensing 8W1E electrodes pre-coated with LR fractions at a final total protein concentration of 20 μg/mL and kept at 37°C in 5% CO<sub>2</sub> and 90% humidity. Attachment of cells on the electrode surface changes the impedance in such a way that morphologic information of the attached cells can be inferred. Capacitance was measured at 40 kHz and 1 V. The time

necessary for EPEC to cover half of the available electrode ( $t_{1/2}$ ) was calculated as previously described.<sup>27</sup>

**Enzyme-Linked Immunosorbent Assay**

IL-8 and keratinocyte-derived chemokine (KC) levels were quantified by using the Quantikine IL-8 immunoassay and KC DuoSet enzyme-linked immunosorbent assay (ELISA) kits (R&D System, Minneapolis, MN).

**Histology**

Distal colonic sections were fixed in 10% formalin and embedded in paraffin. Five-micrometer sections were

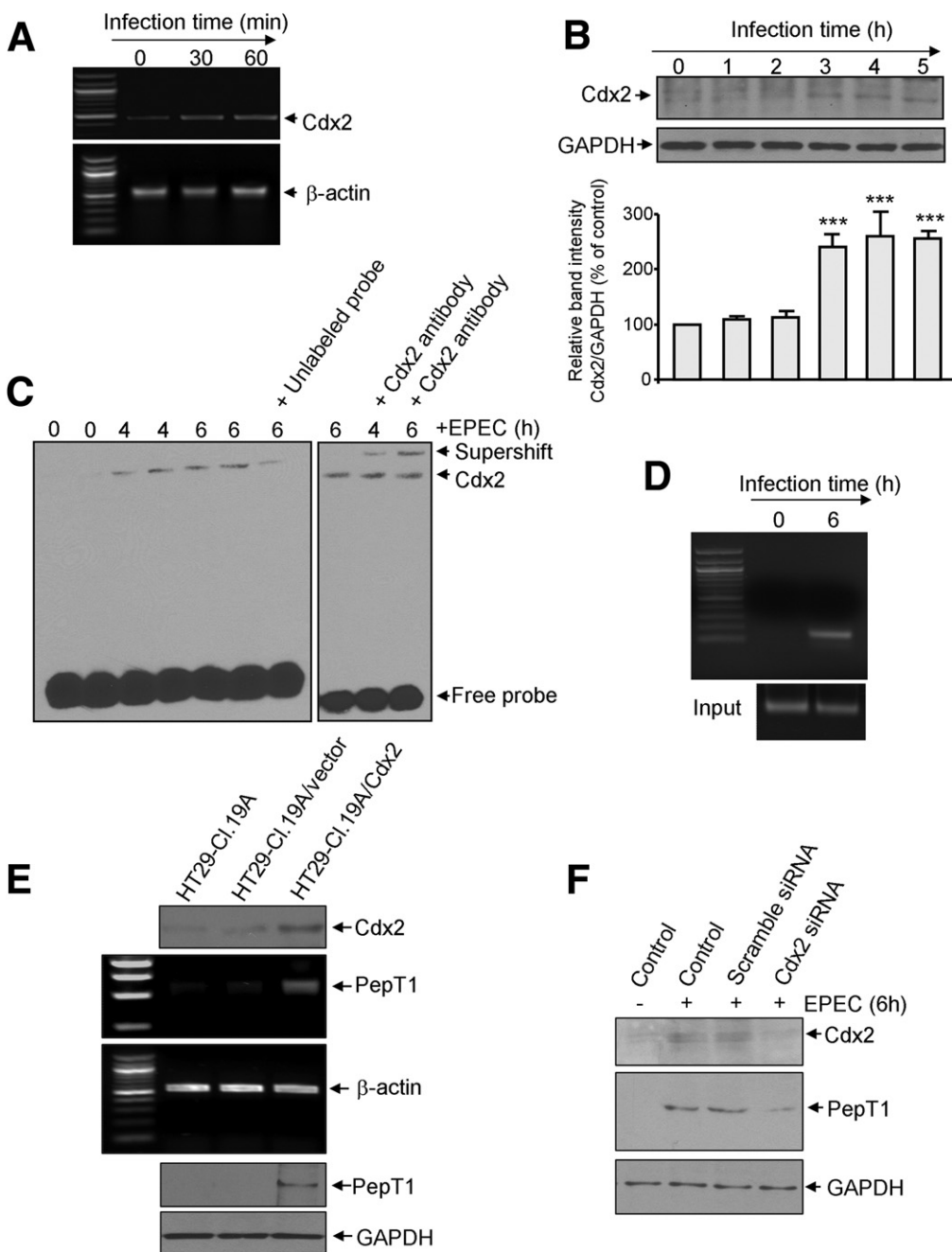


**Figure 2.** Cdx2 is important for EPEC-induced PepT1 expression. HT29-CI.19A cells were infected with EPEC and assessed for Cdx2 expression by RT-PCR (A) and Western blot (B). The binding of Cdx2 to PepT1 promoter was analyzed by EMSA (C) and ChIP assay (D). EMSA was performed using a Cdx2<sup>-579</sup>-specific probe. Specificity of complexes was verified using 200-fold excess of unlabeled probe and by supershift experiment using Cdx2 antibody. ChIP was performed using Cdx2 antibody and Cdx2<sup>-579</sup>-specific primers. (E) Cells were transfected with Cdx2 plasmid (HT29-CI.19A/Cdx2) or the empty vector (HT29-CI.19A/vector). Cdx2 and PepT1 expression levels in wild-type HT29-CI.19A, HT29-CI.19A/Cdx2, and HT29-CI.19A/vector cells were analyzed by RT-PCR and Western blot. (F) HT29-CI.19A cells transfected with scramble or Cdx2 siRNA for 24 hours were infected with EPEC for 6 hours. Cdx2 and PepT1 expression was assessed by Western blot. All experiments were repeated 3 times.

stained with H&E. Photomicrographs were taken using a Nikon Eclipse TS100 microscope (Nikon, Tokyo, Japan).

**Manual Neutrophil Counts**

The number of neutrophils per crypt was counted as previously described.<sup>22</sup>

**Myeloperoxidase Assay**

See Supplementary Materials and Methods.

**Statistical Analysis**

Values are expressed as means ± SEM. Statistical analysis was performed using unpaired 2-tailed Student *t* test by InStat v3.06 (GraphPad, Inc, San Diego, CA) software. *P* < .05 was considered significant.

**Results**

**EPEC Induces PepT1 Promoter Activity and PepT1 Transcription**

Although PepT1 is expressed in inflamed colons,<sup>2,3</sup> the causation factors have not yet been identified. We hypothesized that pathogenic bacteria could induce colonic PepT1 expression. To test this possibility, human

colonic HT29-Cl.19A cells, which do not express a detectable level of PepT1,<sup>2</sup> were infected with EPEC. As shown in Figure 1A and B, EPEC induced PepT1 promoter activity and messenger RNA (mRNA) expression in HT29-Cl.19A cells in a time-dependent manner. The full-length PepT1 cDNA was successfully cloned (GeneBank database accession No ACB71122). In addition, nuclear run-on assays indicated that EPEC strongly induced PepT1 gene transcription in vitro (Figure 1C). Together, these data demonstrate that EPEC transcriptionally induces PepT1 expression in HT29-Cl.19A cells.

**EPEC Induces PepT1 Protein Expression and Transport Activity**

Western blot analysis revealed that EPEC induced a time-dependent increase in PepT1 protein expression in HT29-Cl.19A cells (Figure 1D). The total cellular amount of monocarboxylic transporter-1 (MCT-1), however, was not increased at different time points postinfection, supporting the specificity of the effect of EPEC on PepT1 expression (Figure 1D). Immunofluorescence staining revealed PepT1 expression in EPEC-infected cells, whereas no PepT1 signal was evident in uninfected cells (Figure

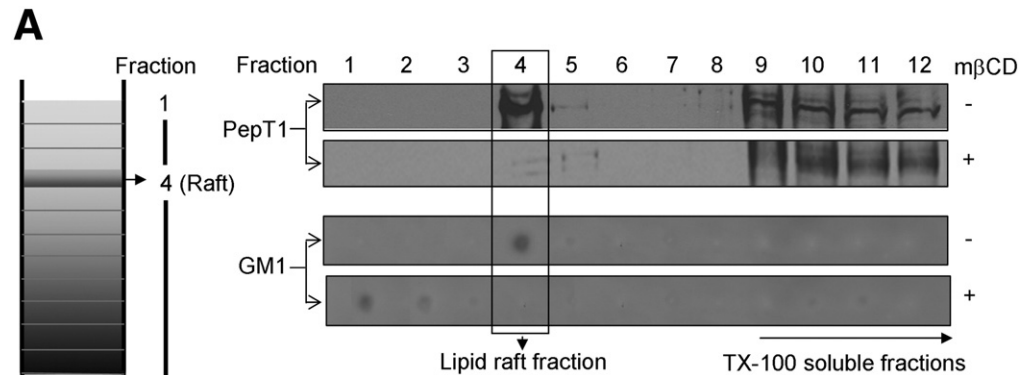
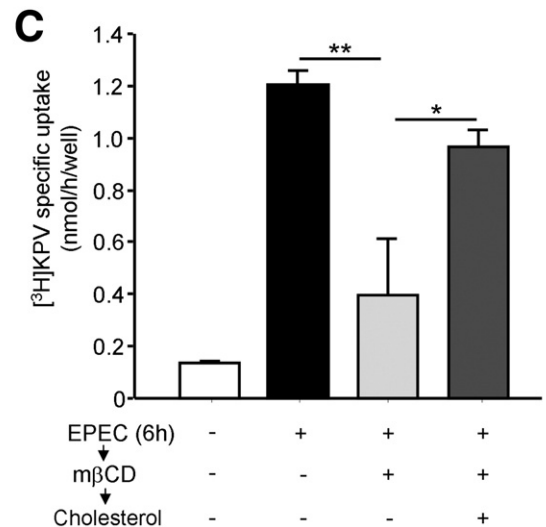
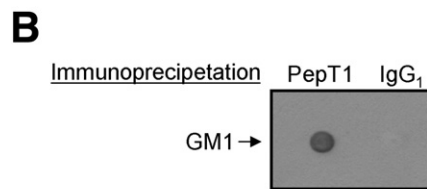


**Figure 3.** EPEC induces PepT1 expression in lipid rafts of HT29-Cl.19A cells. (A) Cells were infected with EPEC for 6 hours, treated or not with 10 mmol/L methyl-β-cyclodextrin (mβCD), lysed, and subjected to sucrose gradient fractionation. Equal total protein amounts of the gradient fractions were analyzed for PepT1 and GM1 distribution by Western blot and dot blot, respectively. (B) EPEC-infected cell lysates were immunoprecipitated using PepT1 antibody or the isotype IgG<sub>1</sub>. Immunoprecipitates were analyzed by dot blot to detect GM1. (C) EPEC-infected cells were treated with mβCD and replenished or not with cholesterol. PepT1-mediated [<sup>3</sup>H]KPV uptake was measured. Values are means ± SEM of 3 determinations. \**P* < .05; \*\**P* < .005.



1E, *i*). Confocal microscopy of polarized HT29-Cl.19A cells at 6 hours postinfection showed that PepT1 was mostly localized in the apical membranes (Figure 1E, *ii*). PepT1-mediated uptake of the tripeptide KPV in HT29-Cl.19A cells was increased after 4 and 6 hours of infection (Figure 1F). Together, these data demonstrate that EPEC induces PepT1 protein expression and transport activity.

### The Transcription Factor Cdx2 Is Crucial for EPEC-Induced PepT1 Expression

Previous studies have suggested that Cdx2 regulates PepT1 expression in IECs.<sup>5,24,28</sup> We next addressed whether Cdx2 mediated EPEC-induced PepT1 expression. EPEC markedly increased Cdx2 mRNA and protein expression in HT29-Cl.19A cells (Figure 2A and 2B). Notably, Cdx2 bound to the human PepT1 promoter at the Cdx2<sup>-579</sup>-binding site as shown by EMSA (Figure 2C). The

loss of the retarded protein-DNA complexes upon addition of an excess of unlabeled probe and their shift in the presence of Cdx2 antibody indicated that the binding of Cdx2 to the PepT1 promoter was sequence specific (Figure 2C). The Cdx2-PepT1 promoter interaction was confirmed by ChIP analysis. As shown in Figure 2D, RT-PCR analysis of the Cdx2 immunoprecipitate derived from infected cells identified a sequence specific to the Cdx2<sup>-579</sup>-binding site, demonstrating the binding of Cdx2 to the PepT1 promoter.

We next investigated whether Cdx2 was directly involved in EPEC-induced PepT1 expression. Figure 2E shows the expression of PepT1 mRNA and protein in HT29-Cl.19A cells overexpressing Cdx2. In contrast, PepT1 expression was not detected in WT HT29-Cl.19A cells or HT29-Cl.19A cells transfected with the empty

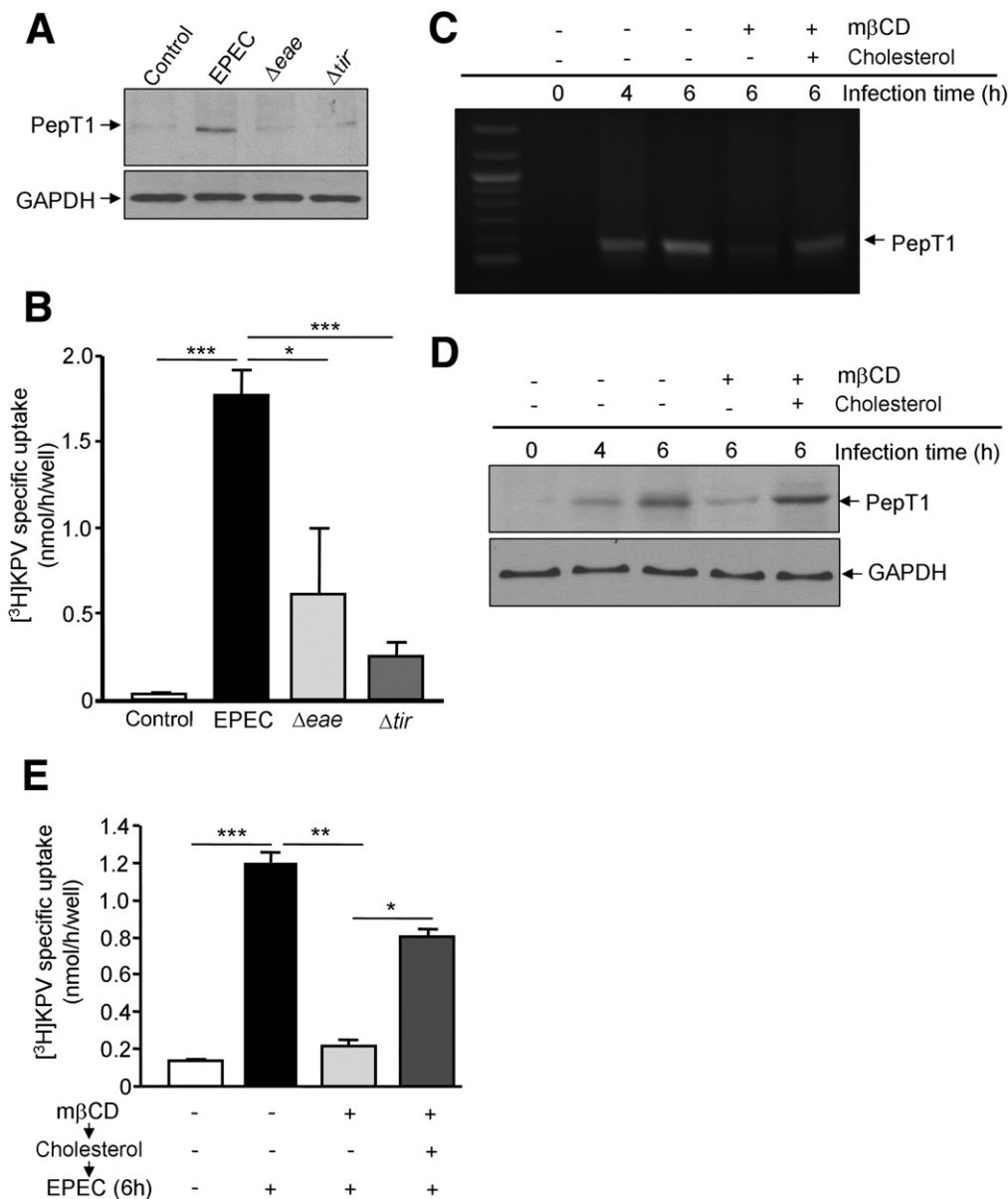


**Figure 4.** EPEC-induced PepT1 expression requires Tir, intimin, and intact host lipid rafts. (A and B) HT29-Cl.19A cells were infected with WT EPEC or EPEC mutants deficient in Tir ( $\Delta tir$ ) or intimin ( $\Delta eae$ ) for 6 hours. Western blot analysis of PepT1 expression (A) and PepT1-mediated [ $^3$ H]KPV uptake (B). (C–E) Cells were treated with 10 mmol/L m $\beta$ CD and replenished or not with 2 mmol/L cholesterol prior to EPEC infection. PepT1 expression and activity were assessed by RT-PCR (C), Western blot (D), and uptake experiments (E). Values are means  $\pm$  SEM of 3 determinations. \* $P < .05$ ; \*\* $P < .005$ ; \*\*\* $P < .001$ .

vector, which exhibited low Cdx2 levels (Figure 2E). Accordingly, silencing of Cdx2 in HT29-Cl.19A cells by Cdx2 small interfering RNA (siRNA) markedly reduced EPEC-induced PepT1 expression (Figure 2F). Together, these results demonstrate the importance of Cdx2 in EPEC-induced PepT1 transcription.

**EPEC Induces PepT1 Expression in LRs**

We previously showed that PepT1 is localized in LRs of IECs.<sup>6</sup> We next addressed whether PepT1 in HT29-Cl.19A cells was also targeted to LRs upon infection with EPEC. Western blot and dot blot analyses revealed that

the levels of PepT1 and of GM1, a well-known LR marker, were increased in LRs compared with other gradient fractions prepared from EPEC-infected cells (Figure 3A). GM1 coimmunoprecipitated with PepT1, but not the isotype IgG<sub>1</sub>, in HT29-Cl.19A cells (Figure 3B). Treatment of infected cells with the cholesterol-disrupting agent mβCD caused most PepT1 and GM1 to move from the LR fraction to high-density fractions (Figure 3A). This change was accompanied by an ~70% decrease in EPEC-induced PepT1 activity, which was recovered by replenishing cell membranes with cholesterol (Figure 3C).

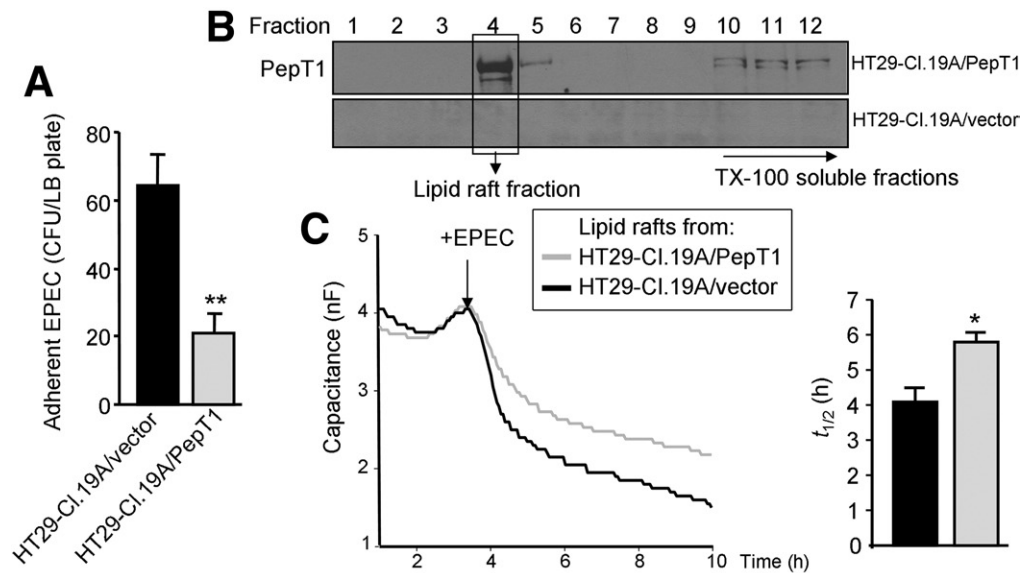
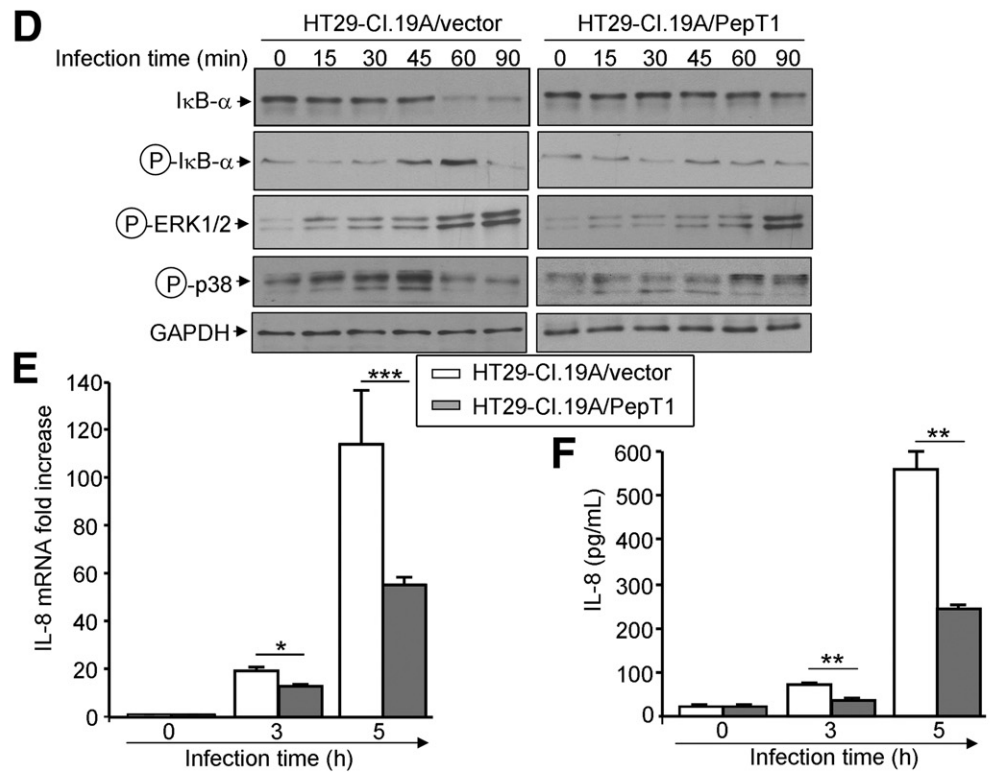


**Figure 5.** PepT1 associated with lipid rafts attenuates EPEC adherence and EPEC-induced inflammation in HT29-Cl.19A cells. (A) EPEC adherence to HT29-Cl.19A cells overexpressing PepT1 (*HT29-Cl.19A/PepT1*) or the empty vector (*HT29-Cl.19A/vector*) at 4 hours postinfection. (B) Western blot analysis for PepT1 distribution in the sucrose-gradient fractions. (C) EPEC adherence to lipid raft-coated electrodes monitored in real time using the electric cell-substrate impedance sensing technique. The time required for EPEC to cover half of the available electrode ( $t_{1/2}$ ) was determined. (D) Degradation of IκB-α and phosphorylation of IκB-α, ERK1/2, and p38 were assessed by Western blot. IL-8 mRNA and protein levels were analyzed by real-time RT-PCR (E) and ELISA (F). Values are means ± SEM of 3 determinations. \* $P < .05$ ; \*\* $P < .005$ ; \*\*\* $P < .001$ .



These results suggest that EPEC induces functional PepT1 expression in the cholesterol-enriched LRs of colonocytes.

**EPEC Induces PepT1 Expression by Intimately Attaching to Host Cells Through LRs**

Tir and intimin are known to be the virulence factors necessary for intimate attachment of EPEC.<sup>11</sup> To investigate whether EPEC-induced PepT1 expression requires the intimate attachment of EPEC to host cells, the effects of EPEC mutants  $\Delta eae$  and  $\Delta tir$ , which are deficient in intimin and Tir expression, respectively, on PepT1 expression were examined. Deficiency in Tir or intimin abrogated the ability of EPEC to induce PepT1 expression and transport activity (Figure 4A and B).

Because LRs have been shown to be important for EPEC adherence and Tir translocation,<sup>29</sup> the possibility that LRs are required for EPEC-induced PepT1 expression was examined. Western blot and RT-PCR analyses showed that m $\beta$ CD treatment markedly reduced EPEC-induced PepT1 mRNA and protein expression in HT29-

Cl.19A cells (Figure 4C and D). In addition, EPEC failed to induce PepT1 transport activity in m $\beta$ CD-treated cells (Figure 4E). Suppression of PepT1 expression and activity by m $\beta$ CD was effectively recovered by membrane cholesterol replenishment (Figure 4C-E). Collectively, these data suggest that EPEC induces PepT1 expression by intimately attaching to host cell membranes through LRs.

**PepT1 Reduces EPEC Adherence and EPEC-Induced Inflammation in Colonocytes**

To elucidate the role of PepT1 associated with LRs in bacterial-epithelial interactions, EPEC adherence to HT29-Cl.19A cells overexpressing PepT1 (HT29-Cl.19A/PepT1) or the empty vector (HT29-Cl.19A/vector) was assessed. A significant decrease in EPEC adherence was evident in HT29-Cl.19A/PepT1 cells compared with HT29-Cl.19A/vector cells (Figure 5A). To examine further the involvement of PepT1 in EPEC adherence, EPEC attachment to the LR fractions prepared from HT29-Cl.19A/PepT1 or HT29-Cl.19A/vector cells was monitored in real time using the electric cell-substrate imped-

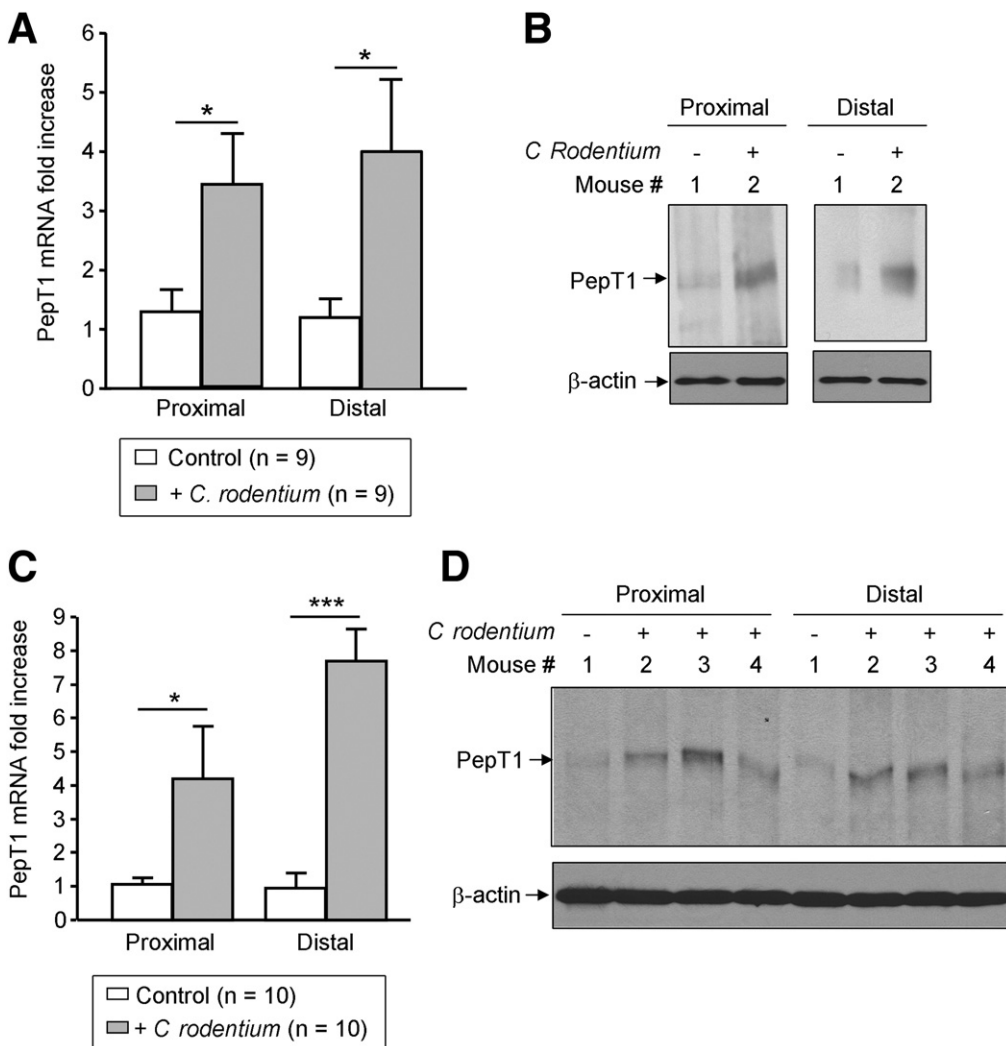


**Figure 6.** *Citrobacter rodentium* induces PepT1 expression in mouse colon. (A and B) Cultured mouse colonic tissues were infected with *C. rodentium* for 6 hours and analyzed for PepT1 expression by real-time RT-PCR (A) and Western blot (B). (C and D) For infection of mice, food was withdrawn, and drinking water was replaced with *C. rodentium* suspension in 20% sucrose distilled water overnight. Mice were killed 7 days after infection. PepT1 expression in mouse colon was analyzed by real-time RT-PCR (C) and Western blot (D). Data are means  $\pm$  SEM. \* $P < .05$ ; \*\*\* $P < .001$ . All experiments were repeated twice with  $n = 9$  (A and B) or  $n = 10$  (C and D) per condition for each experiment.

ance-sensing technique. Figure 5B shows the enrichment of PepT1 in the LR fraction and, to a lesser extent, the Triton X-100-soluble fractions prepared from HT29-Cl.19A/PepT1 cells and its absence in HT29-Cl.19A/vector cells. Attachment of EPEC, assessed by measuring capacitance changes, to LRs from HT29-Cl.19A/PepT1 cells (Figure 5C, grey line) was delayed in comparison with that to LRs from HT29-Cl.19A/vector cells (Figure 5C, black line). The time necessary for EPEC to cover half of the available electrode ( $t_{1/2}$ ) coated with PepT1-containing LRs ( $t_{1/2} = 5.8 \pm 0.25$  hours) was significantly increased compared with that on PepT1-lacking LRs ( $t_{1/2} = 4.1 \pm 0.38$  hours) (Figure 5C). These data suggest that overexpression of PepT1 reduces adherence of EPEC to colonocytes.

The role of PepT1 in EPEC-induced inflammatory responses in colonocytes was next investigated. EPEC induced a stronger and faster  $\text{I}\kappa\text{B-}\alpha$  degradation in HT29-Cl.19A/vector cells compared with HT29-Cl.19A/PepT1 cells (Figure 5D). Furthermore, EPEC-induced phosphorylation of  $\text{I}\kappa\text{B-}\alpha$ , ERK1/2, and p38 kinases was delayed in HT29-Cl.19A/PepT1 cells compared with HT29-Cl.19A/vector cells (Figure 5D). Consistent with these data was a decrease in IL-8 mRNA and protein production in HT29-Cl.19A/PepT1 cells (Figure 5E and F). Together, these findings suggest a role for PepT1 in host defense responses to EPEC infection.

**C rodentium Induces PepT1 Expression in Mouse Colon**

Colonic PepT1 expression upon ex vivo and in vivo infection was examined using *C rodentium*, a murine attaching and effacing pathogen.<sup>18</sup> PepT1 mRNA and protein expression were significantly increased in cultured mouse colonic tissues by 6 hours of infection (Figure 6A and B). Furthermore, colonic PepT1 mRNA and protein expression were induced in mice infected

with *C rodentium* (Figure 6C and D). These results, which are in accordance with in vitro data, suggest that infection with pathogenic bacteria induces PepT1 expression.

**PepT1 Has a Role in the Protective Response in Mouse Colon Against C rodentium**

The role of PepT1 in host responses to *C rodentium* infection was assessed using a PepT1 transgenic mouse model we previously developed.<sup>20</sup> Figure 7A shows a decrease in *C rodentium* adherence to cultured colonic tissues from PepT1 transgenic mice compared with those from WT mice. In addition, cultured colons from PepT1 transgenic mice produced lower mRNA and protein levels of keratinocyte-derived chemokine (KC), a potent murine neutrophil chemoattractant,<sup>30</sup> compared with those from WT mice by 6 hours postinfection (Figure 7B and C).

Consistent with these ex vivo data, colonization of *C rodentium* in colons from PepT1 transgenic mice was reduced compared with those from WT mice (Figure 8A). Furthermore, PepT1 transgenic mice exhibited decreased neutrophil accumulation in the colon, assessed by measuring colonic myeloperoxidase (MPO) activity, compared with WT mice (Figure 8B). Examination of H&E-stained colonic tissues from uninfected mice revealed no morphologic differences between WT and PepT1 transgenic groups (Figure 8C, i). Seven days after *C rodentium* infection, increases in crypt height, an indication of hyperplasia (a distinctive characteristic of *C rodentium* infection<sup>18</sup>), were evident in both WT and PepT1 transgenic mice (Figure 8C, i). There were relatively modest differences in morphology of colons from these mice except for a remarkable decrease in neutrophil infiltration in PepT1 transgenic mice compared with WT mice (Figure 8C, ii), which strongly correlated with the reduction of MPO activity. In addition, compared with WT mice, PepT1 transgenic mice exhibited decreased colonic KC mRNA production and attenuated serum KC levels in response

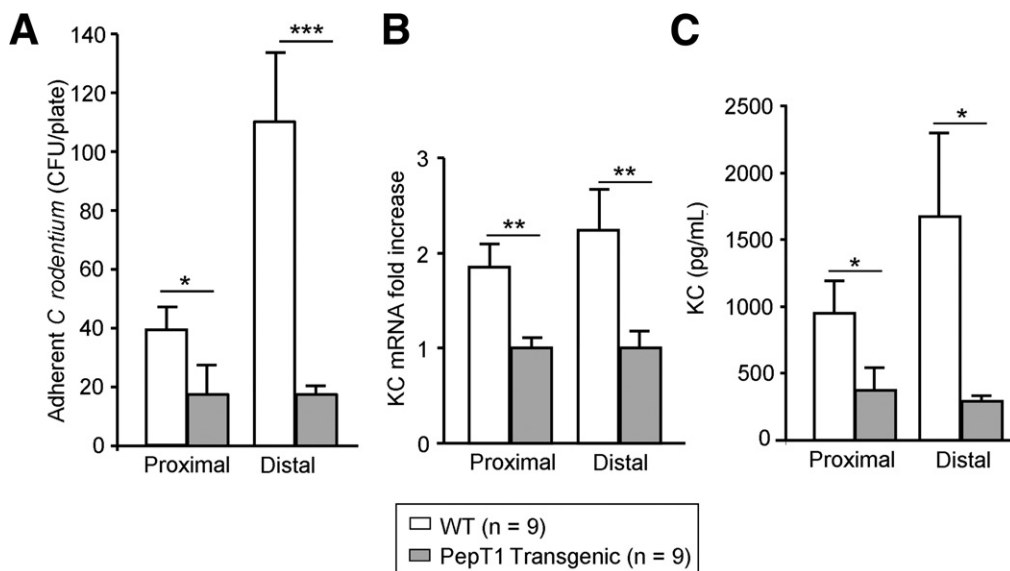
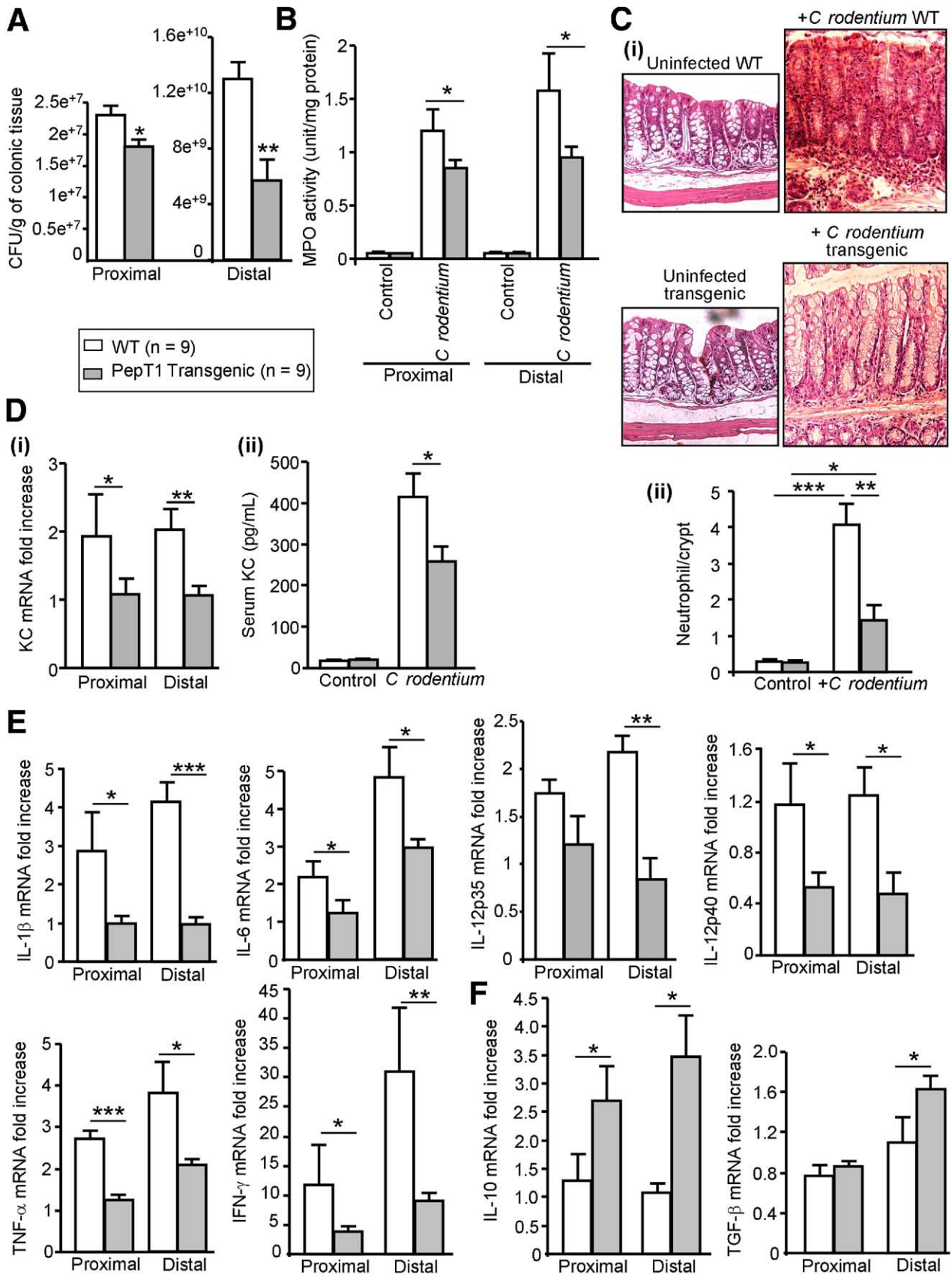


**Figure 7.** PepT1 overexpression reduces *C rodentium* adherence and *C rodentium*-induced cytokine production in cultured mouse colons. Cultured colonic tissues from WT and PepT1 transgenic mice were infected ex vivo with *C rodentium* for 6 hours. (A) *C rodentium* adherence to cultured colonic tissues. KC mRNA and protein levels were determined by real-time RT-PCR (B) and ELISA (C), respectively. Data are means  $\pm$  SEM. \* $P < .05$ ; \*\* $P < .005$ ; \*\*\* $P < .001$ . All experiments were repeated twice with  $n = 9$ /group/condition for each experiment.



to *C rodentium* infection (Figure 8D). Colonic levels of the proinflammatory cytokines IL-1 $\beta$ , IL-6, IL-12, tumor necrosis factor (TNF)- $\alpha$ , and interferon (IFN)- $\gamma$  in PepT1 transgenic mice were also reduced compared with that observed in WT mice (Figure 8E). Production of the anti-inflammatory cytokines IL-10 and transforming growth factor (TGF)- $\beta$  in the colons from PepT1 transgenic mice were increased compared with WT mice (Figure 8F), suggesting that endogenous anti-inflammatory mechanisms might be more effectively activated in PepT1 transgenic mice. Altogether, our data suggest that PepT1 may have a role in colonic infections via modulating bacterial-epithelial interactions and inflammatory response to pathogenic bacteria.

## Discussion

In the present study, we demonstrate that EPEC transcriptionally induces functional PepT1 expression in colonic epithelial cells. Previous studies have shown the effect of EPEC on membrane transport activities in IECs, such as butyrate uptake via monocarboxylic transporter-1<sup>15</sup> and Na<sup>+</sup> transport via Na<sup>+</sup>/H<sup>+</sup> exchange isoforms<sup>16</sup> and Cl<sup>-</sup>/OH<sup>-</sup> exchange.<sup>17</sup> These activity changes have been suggested to be due to the redistribution of surface proteins from the apical membranes into the intracellular compartments.<sup>15,17</sup> The regulation of membrane transporters by EPEC at a transcriptional level has not yet been investigated. Regarding pathogenic effects on PepT1 expression, only one study to date has reported the transcriptional up-regulation of PepT1 in the rat small intestine in response to *Cryptosporidium parvum* infection.<sup>4</sup> Under inflammatory conditions,<sup>2,3</sup> PepT1 expression in the colon has been observed; however, the underlying molecular mechanisms remain unexplored. In an effort to address this, we identified EPEC as a causal factor of PepT1 expression in human colonic HT29-Cl.19A cells, which do not express PepT1 under basal conditions.<sup>2</sup> One of our important findings is that the transcription factor Cdx2 is required for EPEC-induced colonic PepT1 expression, which is in accordance with previous studies showing a role for Cdx2 in the regulation of PepT1 expression in IECs.<sup>5,24,28</sup> With regard to pathologic states, PepT1 expression was detected in the intestinal metaplastic gastric mucosa isolated from transgenic mice with stomach-specific Cdx2 expression.<sup>31</sup> Furthermore, a high correlation exists between PepT1 and Cdx2 expression levels in human gastric tissues develop-

ing intestinal metaplasia.<sup>5</sup> Together, these observations and our findings raise Cdx2 as a key transcription factor in the regulation of PepT1 expression under pathologic conditions. The regulation of Cdx2 especially that is mediated by bacterial pathogen has not been broadly established. Aberrant expression of Cdx2 in *Helicobacter pylori*-associated atrophic gastritis has been reported,<sup>32</sup> but the underlying molecular mechanism is unknown. Recently, bacterial components, such as lipopolysaccharide, were suggested to up-regulate Cdx2 expression via Toll-like receptors 2 and 4 followed by NF- $\kappa$ B activation in cultured biliary epithelial cells and in vivo.<sup>33</sup> Importantly, our study demonstrates that EPEC is a regulator of Cdx2 expression. The signal transduction pathways that are used by EPEC to activate Cdx2, which induces PepT1 expression, are currently under investigation.

We previously showed that PepT1 is localized in LR membrane microdomains,<sup>6</sup> which are known to provide specialized lipid environments to regulate the organization and function of many membrane proteins.<sup>7</sup> Here, we show that EPEC induces PepT1 expression in the LRs of HT29-Cl.19A cells and that the association of PepT1 with LRs can modulate PepT1 transport activity. These findings are of physiologic importance because they demonstrate that PepT1 expressed in colonocytes upon EPEC infection is functionally active.

It has been proposed that, in response to bacterial binding, signaling molecules gather at membrane LR platforms, thereby participating in bacterial adherence and invasion.<sup>8,9</sup> Accordingly, several LR-associated molecules, such as CD44, annexin II, cholesterol, and GPI-anchored proteins are found at EPEC adherent sites.<sup>34,35</sup> Our study demonstrates that EPEC-induced PepT1 expression requires intact LRs, together with the EPEC virulence factors Tir and intimin. Given that the binding of intimin to its receptor Tir is required for the intimate attachment of EPEC to host IECs,<sup>11</sup> we speculate that EPEC induces PepT1 expression by activating signaling via molecules within LRs.

The findings that EPEC-induced PepT1 expression depends on LRs and that PepT1 expressed in colonocytes is functionally targeted to LRs led us to investigate the role of PepT1 associated with LRs in host responses to EPEC virulence. Strikingly, we found that overexpression of PepT1 in HT29-Cl.19A cells markedly reduced EPEC adherence. Furthermore, the presence of PepT1 delayed EPEC attachment to LRs as monitored in real time using

**Figure 8.** PepT1 transgenic mice exhibit decreased susceptibility to *C rodentium* infection compared with WT mice. WT and PepT1 transgenic mice were infected with *C rodentium* and killed at 7 days postinfection. (A) *C rodentium* colonization levels in the colon. (B) Neutrophil infiltration into the colon quantified by measuring MPO activity. (C, i) Representative H&E-stained distal colonic sections. Original magnification, 20 $\times$ . (C, ii) Neutrophils were identified by their distinctive nuclear morphology and counted in 10 crypts per colon. The mean number of neutrophils per crypt was calculated for each colon observed. (D, i) KC mRNA levels in the colon determined by real-time RT-PCR. (D, ii) KC levels in serum determined by ELISA. Colonic mRNA levels of proinflammatory (E) and anti-inflammatory (F) cytokines determined by real-time RT-PCR. Data are means  $\pm$  SEM. \* $P$  < .05; \*\* $P$  < .005; \*\*\* $P$  < .001. All experiments were repeated twice with  $n = 9$ /group/condition for each experiment.

the electric cell-substrate impedance sensing technique. Given the importance of LRs in bacterial adherence to host IECs, these data strongly suggest a potential role for LR-associated PepT1 in bacterial-epithelial interactions. We speculate that the assembly of PepT1 molecules or their interactions with other components inside LRs may result in changes in conformation and/or composition of LRs and, consequently, mollify the binding affinity of EPEC for LRs. Current efforts are centered on studying the spatial distribution of LR proteins upon expression of PepT1, especially those that are required for EPEC infection. Another intriguing finding is that PepT1 attenuates EPEC-triggered proinflammatory responses in IECs as shown by decreases in NF- $\kappa$ B and mitogen-activated protein kinase activation and IL-8 production. Because EPEC-induced IL-8 production in IECs depends on EPEC intimate adherence,<sup>14</sup> the reduction of EPEC-induced inflammation might be a consequence of the decrease in EPEC adherence. Therefore, colonic PepT1 expression might be a host protective mechanism that modulates bacterial-epithelial interaction and inflammatory responses to pathogens.

Our *in vitro* data were convincingly supported by *ex vivo* and *in vivo* studies using *C rodentium* in a mouse model of attaching and effacing pathogen infection.<sup>36</sup> *Ex vivo* experiments showed that *C rodentium* infection strongly enhanced PepT1 mRNA and protein expression in cultured mouse colon. Infection of FVB mice with *C rodentium* also resulted in a massive increase in colonic PepT1 expression. The role of PepT1 expression in the communication of colonic epithelia with *C rodentium* was further supported using a PepT1 transgenic mouse model, which was recently generated and characterized by our group.<sup>20</sup> We found that overexpression of PepT1 in mice reduced colonic colonization of *C rodentium* *ex vivo* and *in vivo*. Remarkably, compared with WT mice, PepT1 transgenic mice exhibited a decrease in *C rodentium*-induced production of the murine CXC chemokine KC and other proinflammatory cytokines in the colon. This may account for the reduction of *C rodentium*-induced neutrophil infiltration into the colon of PepT1 transgenic mice. However, other mechanisms might also be involved because increased colonic anti-inflammatory cytokine production levels were observed in PepT1 transgenic mice, suggesting that endogenous anti-inflammatory mechanisms are more effectively activated in these mice compared with WT mice upon *C rodentium* infection. Together, our studies indicate that PepT1 may participate in modulating bacterial-epithelial interactions and bacteria-induced inflammation. Further studies using other mouse models, such as PepT1 knockout mice, are required to obtain more information about the specific role of PepT1 in colonic responses to bacterial infection.

In conclusion, our study demonstrates that (1) EPEC transcriptionally induces functional PepT1 expression in

LRs of colonocytes, (2) EPEC induces PepT1 expression by intimately attaching to host cell membranes through LRs, (3) transcription factor Cdx2 is crucial for EPEC-induced PepT1 expression, and (4) PepT1 associated with LRs has a role in bacterial-epithelial interaction and bacteria-induced intestinal inflammation. Our findings reveal a novel mechanism underlying the regulation of colonic PepT1 expression/function under pathologic conditions and point out the potential contribution of this transporter to host defense mechanisms in response to pathogen infection.

### Supplementary Data

Note: To access the supplementary material accompanying this article, visit the online version of *Gastroenterology* at [www.gastrojournal.org](http://www.gastrojournal.org), and at doi: [10.1053/j.gastro.2009.06.043](https://doi.org/10.1053/j.gastro.2009.06.043).

### References

- Charrier L, Merlin D. The oligopeptide transporter hPepT1: gateway to the innate immune response. *Lab Invest* 2006;86:538–546.
- Merlin D, Si-Tahar M, Sitaraman SV, et al. Colonic epithelial hPepT1 expression occurs in inflammatory bowel disease: transport of bacterial peptides influences expression of MHC class 1 molecules. *Gastroenterology* 2001;120:1666–1679.
- Ziegler TR, Fernandez-Estivariz C, Gu LH, et al. Distribution of the H<sup>+</sup>/peptide transporter PepT1 in human intestine: up-regulated expression in the colonic mucosa of patients with short-bowel syndrome. *Am J Clin Nutr* 2002;75:922–930.
- Barbot L, Windsor E, Rome S, et al. Intestinal peptide transporter PepT1 is over-expressed during acute cryptosporidiosis in suckling rats as a result of both malnutrition and experimental parasite infection. *Parasitol Res* 2003;89:364–370.
- Shimakura J, Terada T, Shimada Y, et al. The transcription factor Cdx2 regulates the intestine-specific expression of human peptide transporter 1 through functional interaction with Sp1. *Biochem Pharmacol* 2006;71:1581–1588.
- Nguyen HT, Charrier-Hisamuddin L, Dalmasso G, et al. Association of PepT1 with lipid rafts differentially modulates its transport activity in polarized and nonpolarized cells. *Am J Physiol Gastrointest Liver Physiol* 2007;293:G1155–G1165.
- Simons K, Toomre D. Lipid rafts and signal transduction. *Nat Rev Mol Cell Biol* 2000;1:31–39.
- Lafont F, van der Goot FG. Bacterial invasion via lipid rafts. *Cell Microbiol* 2005;7:613–620.
- Manes S, del Real G, Martinez AC. Pathogens: raft hijackers. *Nat Rev Immunol* 2003;3:557–568.
- Nataro JP, Kaper JB. Diarrheagenic *Escherichia coli*. *Clin Microbiol Rev* 1998;11:142–201.
- Nougayrede JP, Fernandes PJ, Donnenberg MS. Adhesion of enteropathogenic *Escherichia coli* to host cells. *Cell Microbiol* 2003;5:359–372.
- Savkovic SD, Koutsouris A, Hecht G. Activation of NF- $\kappa$ B in intestinal epithelial cells by enteropathogenic *Escherichia coli*. *Am J Physiol* 1997;273:C1160–C1167.
- Savkovic SD, Ramaswamy A, Koutsouris A, et al. EPEC-activated ERK1/2 participate in inflammatory response but not tight junction barrier disruption. *Am J Physiol Gastrointest Liver Physiol* 2001;281:G890–G898.
- Czerucka D, Dahan S, Mograbi B, et al. Implication of mitogen-activated protein kinases in T84 cell responses to enteropatho-

- genic *Escherichia coli* infection. *Infect Immun* 2001;69:1298–1305.
15. Borthakur A, Gill RK, Hodges K, et al. Enteropathogenic *Escherichia coli* inhibits butyrate uptake in Caco-2 cells by altering the apical membrane MCT1 level. *Am J Physiol Gastrointest Liver Physiol* 2006;290:G30–G35.
  16. Hecht G, Hodges K, Gill RK, et al. Differential regulation of Na<sup>+</sup>/H<sup>+</sup> exchange isoform activities by enteropathogenic *E coli* in human intestinal epithelial cells. *Am J Physiol Gastrointest Liver Physiol* 2004;287:G370–G378.
  17. Gill RK, Borthakur A, Hodges K, et al. Mechanism underlying inhibition of intestinal apical Cl/OH exchange following infection with enteropathogenic *E coli*. *J Clin Invest* 2007;117:428–437.
  18. Luperchio SA, Schauer DB. Molecular pathogenesis of *Citrobacter rodentium* and transmissible murine colonic hyperplasia. *Microbes Infect* 2001;3:333–340.
  19. Mundy R, MacDonald TT, Dougan G, et al. *Citrobacter rodentium* of mice and man. *Cell Microbiol* 2005;7:1697–1706.
  20. Dalmaso G, Nguyen HT, Sitaraman SV, et al. Generation and characterization of hPepT1 transgenic mice. *FASEB J* 2008;22:1183.6.
  21. Hicks S, Frankel G, Kaper JB, et al. Role of intimin and bundle-forming pili in enteropathogenic *Escherichia coli* adhesion to pediatric intestinal tissue in vitro. *Infect Immun* 1998;66:1570–1578.
  22. Lebeis SL, Bommarium B, Parkos CA, et al. TLR signaling mediated by MyD88 is required for a protective innate immune response by neutrophils to *Citrobacter rodentium*. *J Immunol* 2007;179:566–577.
  23. Wei OL, Hilliard A, Kalman D, et al. Mast cells limit systemic bacterial dissemination but not colitis in response to *Citrobacter rodentium*. *Infect Immun* 2005;73:1978–1985.
  24. Nduati V, Yan Y, Dalmaso G, et al. Leptin transcriptionally enhances peptide transporter (hPepT1) expression and activity via the cAMP-response element-binding protein and Cdx2 transcription factors. *J Biol Chem* 2007;282:1359–1373.
  25. Nguyen HT, Amine AB, Lafitte D, et al. Proteomic characterization of lipid rafts markers from the rat intestinal brush border. *Biochem Biophys Res Commun* 2006;342:236–244.
  26. Dalmaso G, Charrier-Hisamuddin L, Thu Nguyen HT, et al. PepT1-mediated tripeptide KPV uptake reduces intestinal inflammation. *Gastroenterology* 2008;134:166–178.
  27. Wegener J, Keese CR, Giaever I. Electric cell-substrate impedance sensing (ECIS) as a noninvasive means to monitor the kinetics of cell spreading to artificial surfaces. *Exp Cell Res* 2000;259:158–166.
  28. Dalmaso G, Nguyen HT, Yan Y, et al. Butyrate transcriptionally enhances peptide transporter PepT1 expression and activity. *PLoS ONE* 2008;3:e2476.
  29. Allen-Vercoe E, Waddell B, Livingstone S, et al. Enteropathogenic *Escherichia coli* Tir translocation and pedestal formation requires membrane cholesterol in the absence of bundle-forming pili. *Cell Microbiol* 2006;8:613–624.
  30. Kobayashi Y. Neutrophil infiltration and chemokines. *Crit Rev Immunol* 2006;26:307–316.
  31. Mutoh H, Satoh K, Kita H, et al. Cdx2 specifies the differentiation of morphological as well as functional absorptive enterocytes of the small intestine. *Int J Dev Biol* 2005;49:867–871.
  32. Satoh K, Mutoh H, Eda A, et al. Aberrant expression of CDX2 in the gastric mucosa with and without intestinal metaplasia: effect of eradication of *Helicobacter pylori*. *Helicobacter* 2002;7:192–198.
  33. Ikeda H, Sasaki M, Ishikawa A, et al. Interaction of Toll-like receptors with bacterial components induces expression of CDX2 and MUC2 in rat biliary epithelium in vivo and in culture. *Lab Invest* 2007;87:559–571.
  34. Goosney DL, DeVinney R, Finlay BB. Recruitment of cytoskeletal and signaling proteins to enteropathogenic and enterohemorrhagic *Escherichia coli* pedestals. *Infect Immun* 2001;69:3315–3322.
  35. Zobiack N, Rescher U, Laarmann S, et al. Cell-surface attachment of pedestal-forming enteropathogenic *E coli* induces a clustering of raft components and a recruitment of annexin 2. *J Cell Sci* 2002;115:91–98.
  36. Borenshtein D, Nambiar PR, Groff EB, et al. Development of fatal colitis in FVB mice infected with *Citrobacter rodentium*. *Infect Immun* 2007;75:3271–3281.

---

Received March 16, 2009. Accepted June 11, 2009.

#### Reprint requests

Address requests for reprints to: Hang Thi Thu Nguyen, PhD, Emory University, Department of Medicine, 615 Michael Street, Atlanta, Georgia 30322. e-mail: [hnguye9@emory.edu](mailto:hnguye9@emory.edu); fax: (404) 727-5767.

#### Acknowledgments

The authors thank Dr Jan Michael Klapproth (Emory University) for kindly providing bacterial strains, Dr Sarah Lebeis and Maiko Sasaki for their technical advice, and Dr Tracy Obertone for careful editing of this manuscript.

H.T.T.N. and G.D. contributed equally to this work.

#### Conflicts of interest

The authors disclose no conflicts.

#### Funding

Supported by National Institutes of Health of Diabetes and Digestive and Kidney Diseases (research center grant R24-DK064399, grant R01-DK061941-02 [to D.M.], and R01-DK06411 [to S.V.S.]), National Institute of Allergy and Infectious Diseases (grant R01AI056067 [to K.M.]) and the Crohn's and Colitis Foundation of America (research fellowship award [to G.D.]).

## Supplementary Materials and Methods

### Experimental Animals

In all experiments, 8-week-old FVB mice were used. FVB mice, which possess advantageous features for transgenic mouse generation and study,<sup>1</sup> were used to generate PepT1 transgenic mice as we previously described.<sup>2</sup> All mice were group housed in standard cages under a controlled temperature (25°C) and photoperiod (12:12-hour light/dark cycle) and were allowed standard chow and tap water ad libitum. All procedures using mice were in accordance with the Emory University Institutional Animal Care.

### RNA Extraction, Reverse-Transcription Polymerase Chain Reaction, and Real-Time Reverse-Transcription Polymerase Chain Reaction

Total RNA was extracted using TRIzol (Invitrogen, Grand Island, NY) and reverse transcribed using cDNA Synthesis kit (Fermentas, Glen Burnie, MD). Reverse-transcription polymerase chain reaction (RT-PCR) was performed using GeneJET Fast PCR kit (Fermentas) and specific primers: human PepT1 sense 5'-CGC CAT GGG AAT GTC CAA ATC ACA CAG T-3', human PepT1 antisense 5'-CAT CTG TTT CTG TGA ATT GGC CCC-3';  $\beta$ -actin sense 5'-GTC ACC CAC ACT GTG CCC ATC-3',  $\beta$ -actin antisense 5'-ACG GAG TAC TTG CGC TCA GGA-3'.

Real-time RT-PCR was performed using an iCycler (Bio-Rad, Hercules, CA). Briefly, complementary DNA (cDNA) was amplified by 40 cycles of 95°C-15 seconds and 60°C-1 minute, using the iQ SYBR Green Supermix (Bio-Rad) and specific primers: mouse PepT1 sense 5'-CGT GCA AGT AGC ACT GTC CAT-3', mouse PepT1 antisense 5'-GGC TTG ATT CCT CCT GTA CCA-3'; interleukin (IL)-8 sense 5'-GTG CAG TTT TGC CAA GGA GT-3', IL-8 antisense 5'-AAA TTT GGG GTG GAA AGG TT-3'; keratinocyte-derived chemokine (KC) sense 5'-TTG TGC GAA AAG AAG TGC AG-3', KC antisense 5'-TAC AAA CAC AGC CTC CCA CA-3'; IL-1 $\beta$  sense 5'-TCG CTC AGG GTC ACA AGA AA-3', IL-1 $\beta$  antisense 5'-CAT CAG AGG CAA GGA GGA AAA C-3'; IL-6 sense 5'-ACA AGT CGG AGG CTT AAT TAC ACA T-3', IL-6 antisense 5'-TTG CCA TTG CAC AAC TCT TTT C-3'; IL-12p40 sense 5'-GGA AGC ACG GCA GCA GAA TA-3', IL-12p40 antisense 5'-AAC TTG AGG GAG AAG TAG GAA TGG-3'; IL-12p35 sense 5'-TAC TAG AGA GAC TTC TTC CAC AAC AAG AG-3', IL-12p35 antisense 5'-TCT GGT ACA TCT TCA AGT CCT CAT AGA-3'; tumor necrosis factor (TNF)- $\alpha$  sense 5'-AGG CTG CCC CGACTA CGT-3', TNF- $\alpha$  antisense 5'-GAC TTT CTC CTG GTA TGA GAT AGC AAA-3'; interferon (IFN)- $\gamma$  sense 5'-CAG CAA CAG CAA GGC GAA A-3', IFN- $\gamma$  antisense 5'-CTG GAC CTG TGG GTT GTT GAC-3'; IL-10 sense 5'-GGT TGC CAA GCC TTA TCG GA-3', IL-10 antisense 5'-ACC TGC TCC ACT GCC TTG CT-3';

transforming growth factor (TGF)- $\beta$  sense 5'-TGCGCT-TGCAGAGATTAATAA-3', TGF- $\beta$  antisense 5'-AGA-CAGCCACTCAGGCGTAT-3'; 18S sense 5'-CCC CTC GAT GAC TTT AGC TGA GTG T-3', 18S antisense 5'-CGC CGG TCC AAG AAT TTC ACC TCT-3'; mouse 36B4 sense 5'-TCC AGG CTT TGG GCA TCA-3', mouse 36B4 antisense 5'-CTT TAT CAG CTG CAC ATC ACT CAG A-3'. 18S and 36B4 were used as housekeeping genes. Fold induction was calculated using the threshold cycle (Ct) method:  $\Delta\Delta\text{CT} = (\text{Ct}_{\text{Target}} - \text{Ct}_{\text{housekeeping}})_{\text{infected}} - (\text{Ct}_{\text{Target}} - \text{Ct}_{\text{housekeeping}})_{\text{uninfected}}$ , and the final data were derived from  $2^{-\Delta\Delta\text{CT}}$ .

### Cloning of Full-Length cDNA Encoding PepT1 Expressed in Enteropathogenic Escherichia coli-Infected HT29-Cl.19A Cells

RT-PCR was performed using specific primers: sense 5'-CGC CAT GGG AAT GTC CAA ATC-3', antisense 3'-CCC CGG TTA AGT GTC TTT GTC TAC-5'. After an initial denaturation at 94°C for 5 minutes, PCR was performed for 35 cycles (denaturation 94°C-1 minute, annealing 60°C-30 seconds, and extension 72°C-3 minutes), followed by a final extension at 72°C for 10 minutes.

### Electrophoretic Mobility Shift Assay

Cdx2-DNA binding was analyzed in cellular extracts prepared in totex buffer (20 mmol/L HEPES, pH 7.9, 350 mmol/L NaCl, 20% glycerol, 1% NP-40, 1 mmol/L MgCl<sub>2</sub>, 0.5 mmol/L EDTA, 0.1 mmol/L EGTA). Samples (5  $\mu$ g) were incubated for 20 minutes at room temperature with a biotin-labeled, double-stranded oligonucleotide encoding the Cdx2<sup>-579</sup>-binding site-containing PepT1 promoter. Complexes were resolved by electrophoresis on 5% Tris-Borate-EDTA (TBE) gels. Gels were transferred to Bio-dyne B Nylon Membranes (Pierce, Rockford, IL), and complexes were visualized using the Chemiluminescent Nucleic Acid Detection System (Pierce). Specificity of the complexes was analyzed by incubation with a 200-fold excess of unlabeled oligonucleotides. Supershift assay was performed using 2  $\mu$ g of Cdx2 antibody (Zymed Laboratories, San Francisco, CA).

### Chromatin Immunoprecipitation Assay

Chromatin immunoprecipitation (ChIP) was performed using a ChIP kit (Upstate, Lake Placid, NY). Briefly, after protein-DNA cross-linking, cells were lysed and sonicated, and the supernatant was precleared with protein A-agarose/salmon sperm DNA to reduce the non-specific background. The samples were then immunoprecipitated using Cdx2 antibody. The complexes were collected in protein A-agarose/salmon sperm DNA slurry and washed. The immunoprecipitated chromatin was eluted from the protein A, and the cross-linked protein-DNA complexes were reversed. The DNA was purified by incubation with proteinase K, followed by phenol/chlo-

roform extraction and ethanol precipitation. Cdx2 promoter elements were detected by PCR using specific primers: Cdx<sup>579</sup> sense 5'-TCT TAA AGA AAG GAA ATG TAG AAT CC-3', Cdx<sup>579</sup> antisense 5'-TGT GTG TGT GAA TGA GGA TTG A-3'.

#### ***Nuclear Run-on Assay***

Five  $\times 10^7$  nuclei isolated as previously described<sup>3</sup> were incubated at 30°C for 20 minutes in 300  $\mu$ L transcription buffer (5 mmol/L Tris-HCl, pH 8.0; 2.5 mmol/L MgCl<sub>2</sub>; 150 mmol/L KCl; 0.25 mmol/L each of adenosine triphosphate, guanosine triphosphate, cytidine triphosphate, and uridine triphosphate). The reaction was stopped by addition of 30  $\mu$ L of 10 mmol/L CaCl<sub>2</sub> and 20  $\mu$ L of 8.5 mg/mL DNase I for 15 minutes at 37°C. The mixture was deproteinized with 20  $\mu$ g/mL proteinase K for 45 minutes at 37°C. After RNA precipitation, cDNA was synthesized and used for RT-PCR using specific primers: hPepT1 sense 5'-CGC CAT GGG AAT GTC CAA ATC ACA CAG T-3', hPepT1 antisense 5'-CAT CTG TTT CTG TGA ATT GGC CCC-3';  $\beta$ -actin sense 5'-GTC ACC CAC ACT GTG CCC ATC-3',  $\beta$ -actin antisense 5'-ACG GAG TAC TTG CGC TCA GGA-3'.

#### ***Western Blot and Dot Blot***

Total and membrane proteins were extracted as previously described.<sup>4</sup> Total cell lysates or gradient fractions extracted from HT29-Cl.19A were resolved on 10% polyacrylamide gels and transferred to nitrocellulose membranes (Bio-Rad, Hercules, CA). Membranes were probed with relevant antibodies followed by incubation with appropriate horseradish peroxidase-conjugated secondary antibodies (Amersham Biosciences, Piscataway, NY). Blots were detected using the Enhanced Chemiluminescence Detection kit (Amersham Biosciences).

To detect ganglioside GM1 in the gradient fractions, 2  $\mu$ g of protein from each fraction was spotted on nitro-

cellulose membranes. Membranes were blocked, washed as described above for Western blot analysis, and then incubated with horseradish peroxidase-conjugated cholera toxin B (CTB; Sigma). Blots were developed as described above.

#### ***Myeloperoxidase Assay***

Colonic tissue samples were homogenized in ice-cold potassium phosphate buffer (50 mmol/L K<sub>2</sub>HPO<sub>4</sub> and 50 mmol/L KH<sub>2</sub>PO<sub>4</sub> [pH 6.0]) containing 0.5% hexadecyltrimethylammonium bromide (Sigma). The homogenates were then sonicated, freeze-thawed for 3 cycles, and centrifuged at 14,000 rpm for 15 minutes. Supernatants or myeloperoxidase standard (20  $\mu$ L) were added to 200  $\mu$ L of substrate (0.167 mg *o*-dianisidine hydrochloride [Sigma] per milliliter H<sub>2</sub>O, 0.0005% H<sub>2</sub>O<sub>2</sub>, in potassium phosphate buffer), and the change in absorbance at 450 nm was measured. Myeloperoxidase was expressed as units per milligram of protein, where 1 unit was defined as the amount that degrades 1  $\mu$ mol of H<sub>2</sub>O<sub>2</sub> per minute.

#### **References**

1. Taketo M, Schroeder AC, Mobraaten LE, et al. FVB/N: an inbred mouse strain preferable for transgenic analyses. *Proc Natl Acad Sci U S A* 1991;88:2065-2069.
2. Dalmaso G, Nguyen HTT, Sitaraman SV, et al. Generation and characterization of hPepT1 transgenic mice. *FASEB J* 2008;22:1183.6.
3. Cuff MA, Lambert DW, Shirazi-Beechey SP. Substrate-induced regulation of the human colonic monocarboxylate transporter, MCT1. *J Physiol* 2002;539:361-371.
4. Nduati V, Yan Y, Dalmaso G, et al. Leptin transcriptionally enhances peptide transporter (hPepT1) expression and activity via the cAMP-response element-binding protein and Cdx2 transcription factors. *J Biol Chem* 2007;282:1359-1373.